PNAS
www.pnas.org

Supplementary Information for
A multi-omic study uncovers bZIP23-PER1A-mediated detoxification pathway to enhance seed vigor in rice

Wei-Qing Wang[1], Ding-Yi Xu[1], Ya-Ping Sui[1,2], Xiao-Hui Ding[1,2], Xian-Jun Song[1,3*]

Xian-Jun Song
Email: songxj@ibcas.ac.cn

This PDF file includes:

Figs. S1 to S26
Tables S1 to S7
Legends for Datasets S1 to S7
SI References

Other supplementary materials for this manuscript include the following:

Datasets S1 to S7

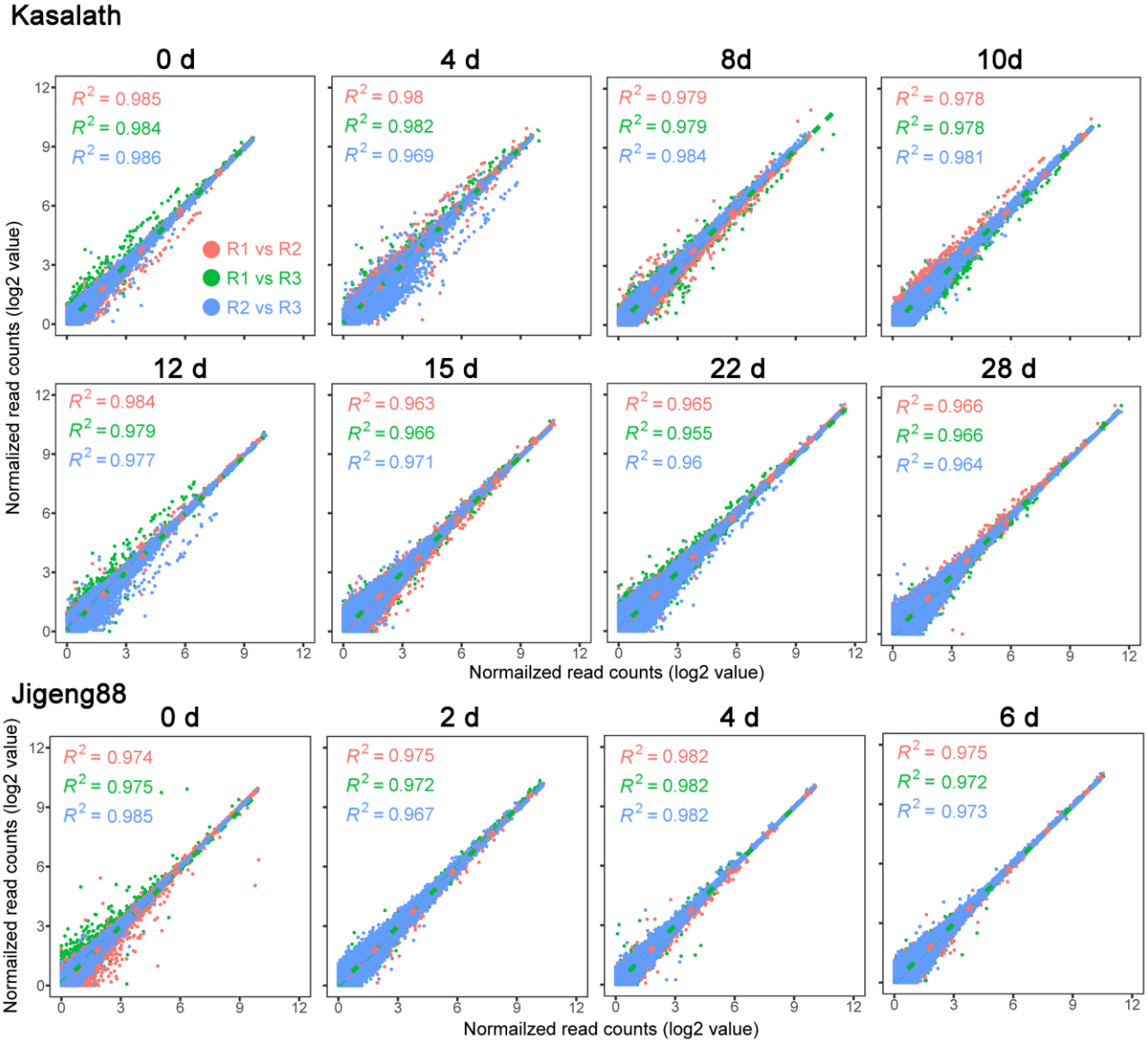

Fig. S1. Correlation of expression between replications at each ageing time points. Different colors indicate the paired comparison between different two replicates at each time points of ageing.

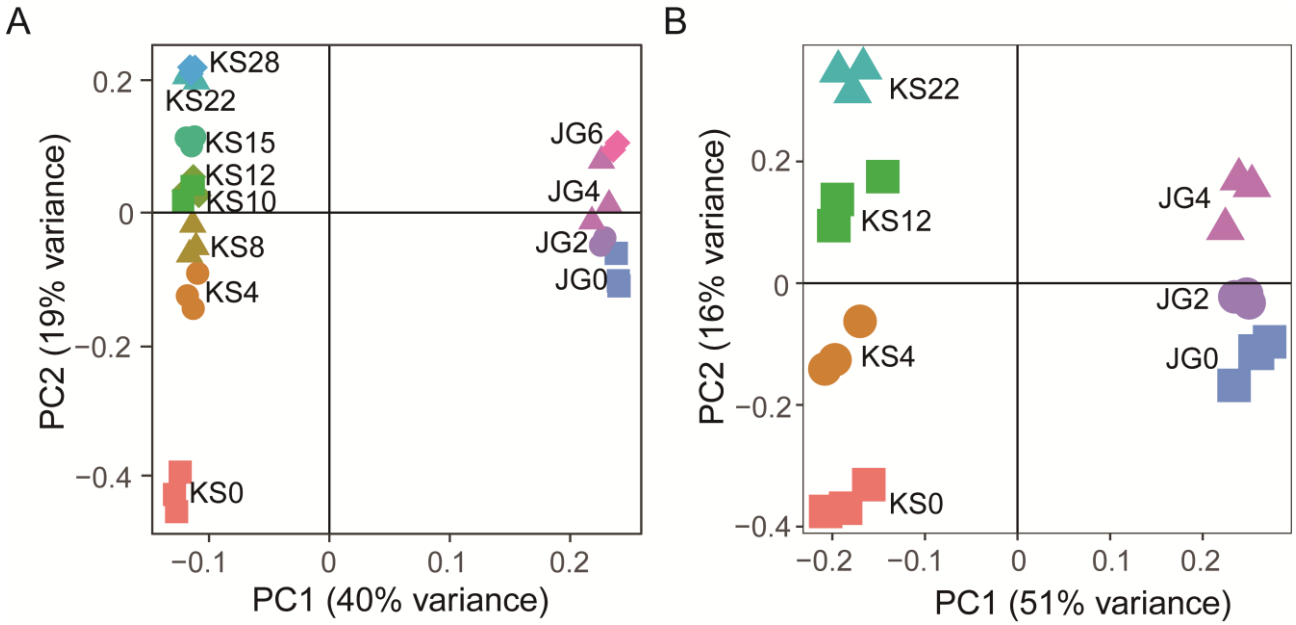

Fig. S2. Principal component analysis (PCA) of gene expression and metabolite accumulation from Kasalath and Jigeng88 seeds aged for different periods of time. (*A*) PCA of gene expression. (*B*) PCA of metabolite accumulation. KS, represents Kasalath rice, JG represents Jigeng88 rice, and the numbers following KS and JG represent the ageing time (days).

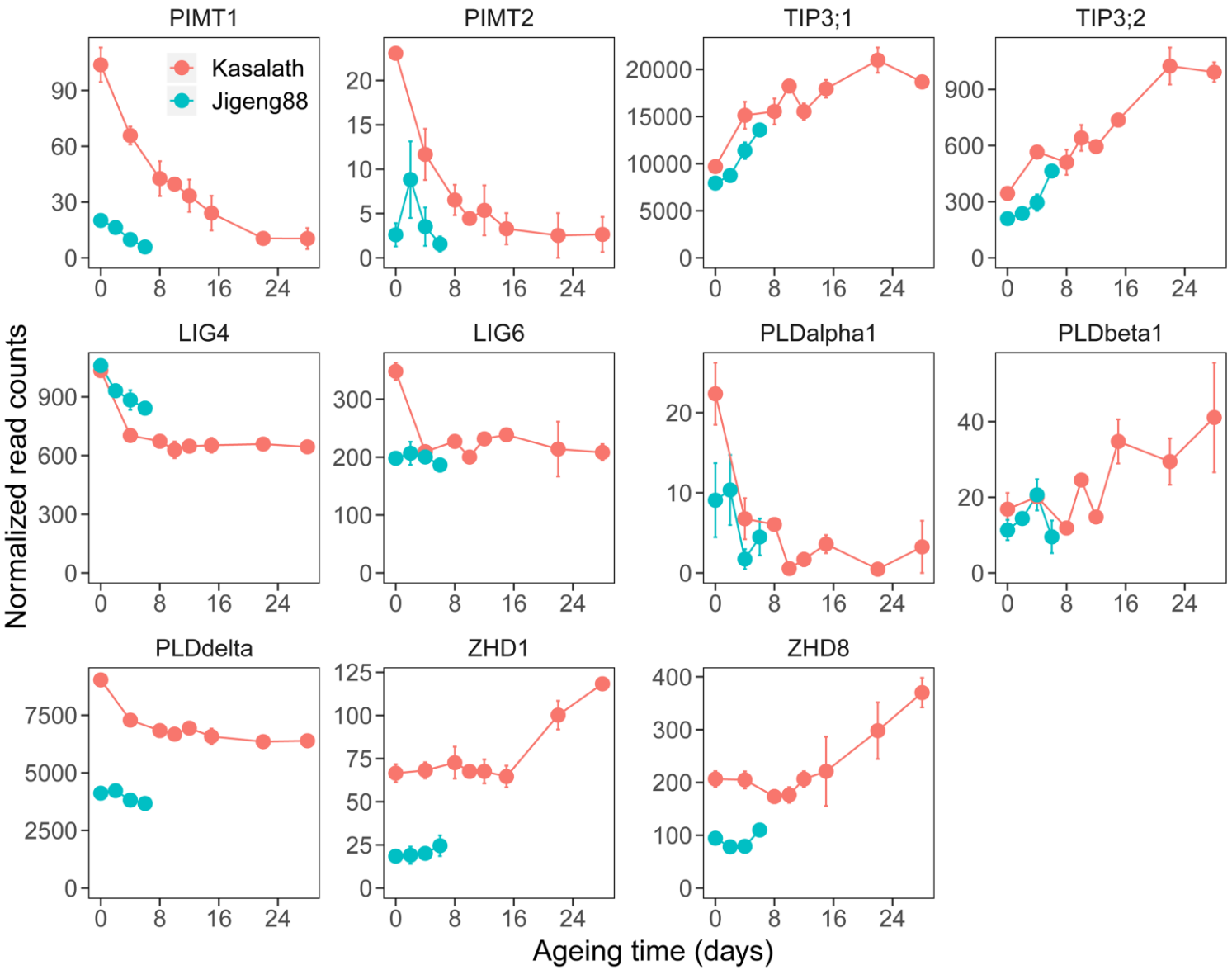

Fig. S3. Expression of genes reported to be involved in rice seed longevity or homologous to those associated with seed longevity in other species. Read counts are normalized across all the samples from Kasalath and Jigeng88 seeds using DESeq2 program. Error bars indicate ±se (n = 3). PIMT, protein-L-isoaspartate O-methyltransferase; TIP, tonoplast intrinsic protein; LIG, DNA ligase; PLD, phospholipase; ZHD, ZF-HD homeobox protein.

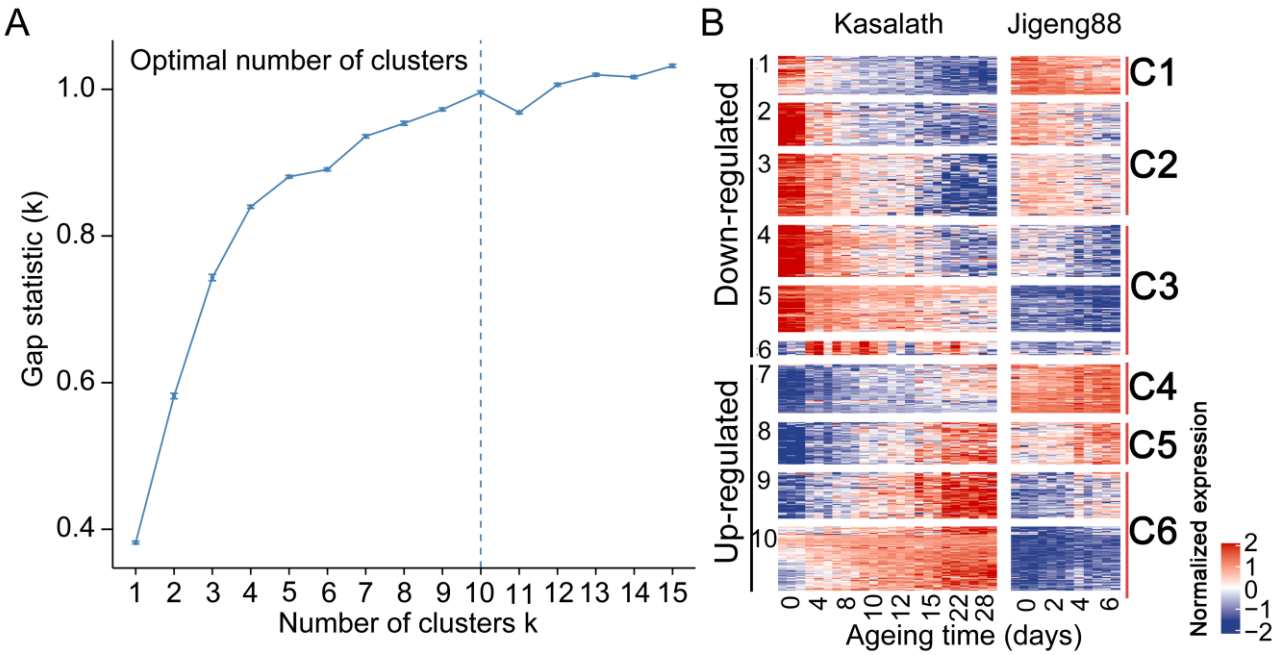

Fig. S4. K-Means cluster of differentially expressed (DE) transcripts during Kasalath seed ageing. (*A*) Determining optimal number of clusters for K-Means clustering. Expression of DE transcripts during Kasalath seed ageing were compared to those during Jigeng88 seed ageing and the optimal number of clusters were determined using the factoextra package embedded in R. Dashed line indicates the optimal number of clusters. (*B*) Heat map showing the expression of DE transcripts of each cluster. Numbers of 1 to 10 in the left panel were the clusters estimating from the K-Means clustering. The clusters were further grouped into C1 to C6 (at right side of the panel) in manual based upon trend of change in expressionduring Kasalath seed ageing (down-regulated or up-regulated) and the abundance of transcripts in Kasalath seeds compared to those in Jigeng88 seeds.

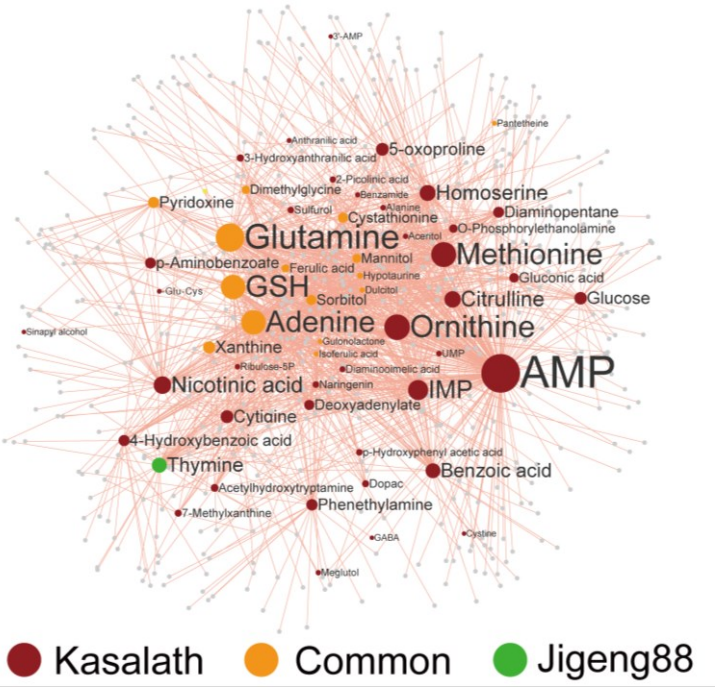

Fig. S5. Predicted metabolic network associated with DA metabolites. Colored bubbles are the metabolites DA during Kasalath and/or Jigeng88 seed ageing and grey bubbles are the metabolites with association predicted from the MetaboAnalyst database. Deep red, orange and green bubbles represent the metabolites DA during Kasalath, both two varieties and Jigeng88 seed ageing, respectively. Bubbles and metabolite names were plotted in different size according to the number of associated metabolites. GSH, glutathione.; AMP, adenosine monophosphate.

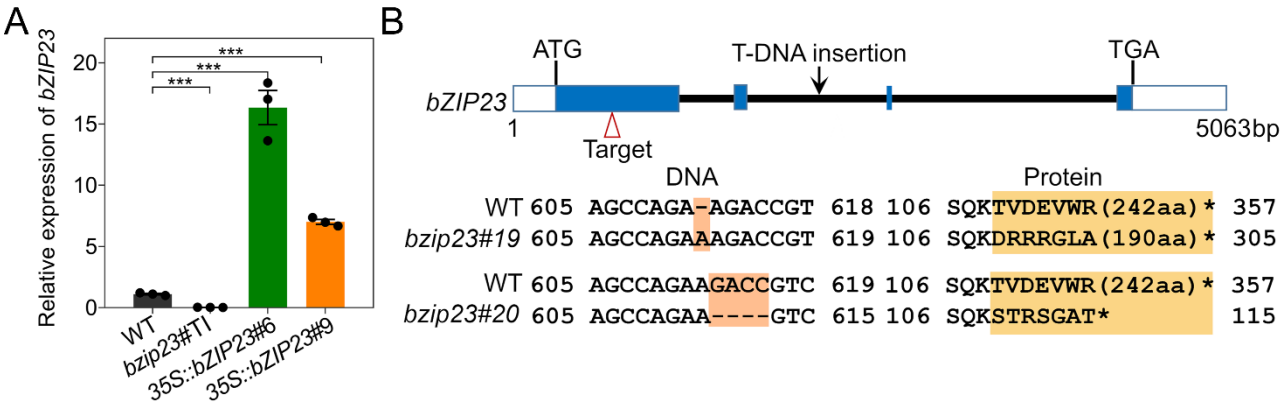

Fig. S6. Genetic modification of *bZIP23* in rice. (*A*) Expression of *bZIP23* in seeds of wild type (WT), *bZIP23* T-DNA insertion (*bzip23*#TI) and over-expression transgenic (*35S:bZIP23*#6 and *35S:bZIP23*#9) plants. Seeds of *bZIP23* T-DNA insertion was provided by Prof. Xiong and the diagram for mutation was shown in (*B*). ***, $p < 0.001$ (unpaired t-test). Error bars indicate ±se (n = 3). (*B*) Schematic diagram showing *bZIP23* mutation mediated by CRISPR/Cas9. Blue filled and blank boxes indicate cDNA and UTR regions, respectively; black line shows intron region. Red triangle shows the target of sgRNA genes. Editing sites on *bZIP23* DNA and protein sequence are indicated with orange and yellow boxes, respectively. The omitted amino acids (aa) are indicated in the parenthesis; *, stop codon.

Fig. S7. Schematic diagram showing *bZIP42* mutation mediated by CRISPR/Cas9. Blue filled and blank boxes indicate cDNA and UTR regions, respectively; black line shows intron region. Red triangle shows the target of sgRNA genes. Editing sites on *bZIP42* DNA and protein sequence are indicated with orange and yellow boxes, respectively. The omitted amino acids (aa) are indicated in the parenthesis; *, stop codon.

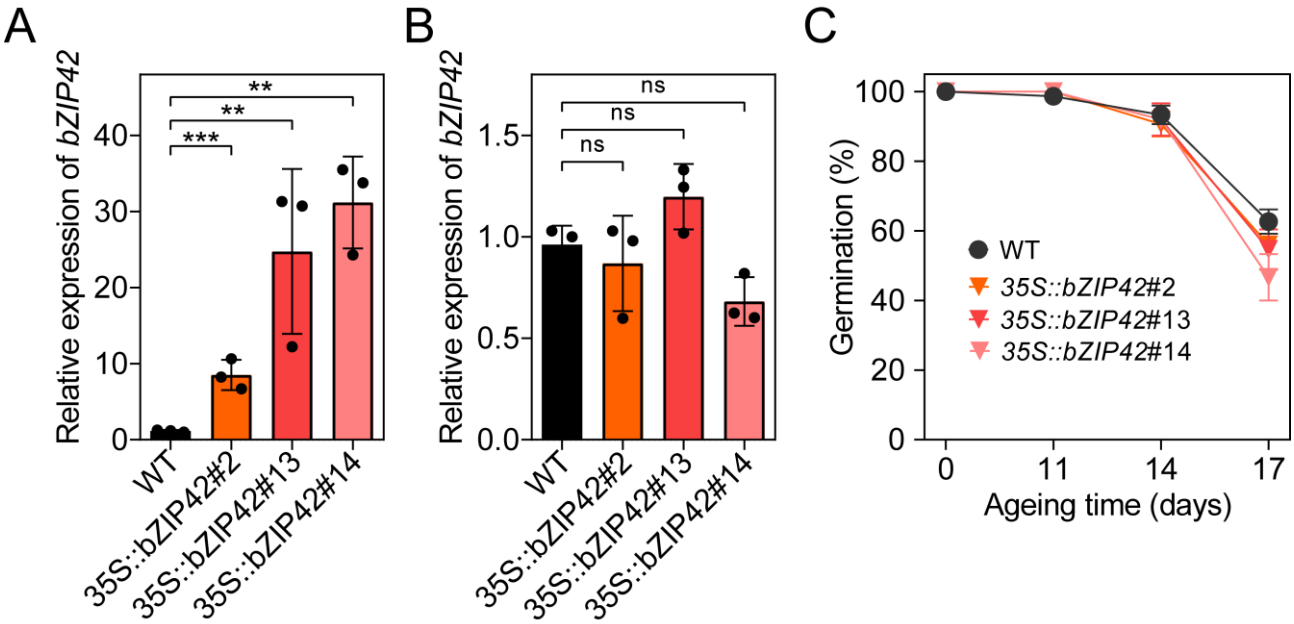

Fig. S8. Overexpression of *bZIP42* in rice. (*A*) Expression of *bZIP42* in leaves of wild type (WT) and over-expression transgenic (*35S:: bZIP42*#2, *35S:: bZIP42*#13 and *35S:: bZIP42*#14) plants. (*B*) Expression of *bZIP42* in seeds of wild type (WT) and over-expression transgenic (*35S::bZIP42*#2, *35S::bZIP42*#13 and *35S::bZIP42*#14) plants. **, $p < 0.01$, ***, $p < 0.001$ (unpaired t-test). (*C*) Change of seed germination of wild type (WT) and over-expression transgenic (*35S::bZIP42*#2, *35S::bZIP42*#13 and *35S::bZIP42*#14) plants during seed ageing. Error bars indicate ±se (n = 3).

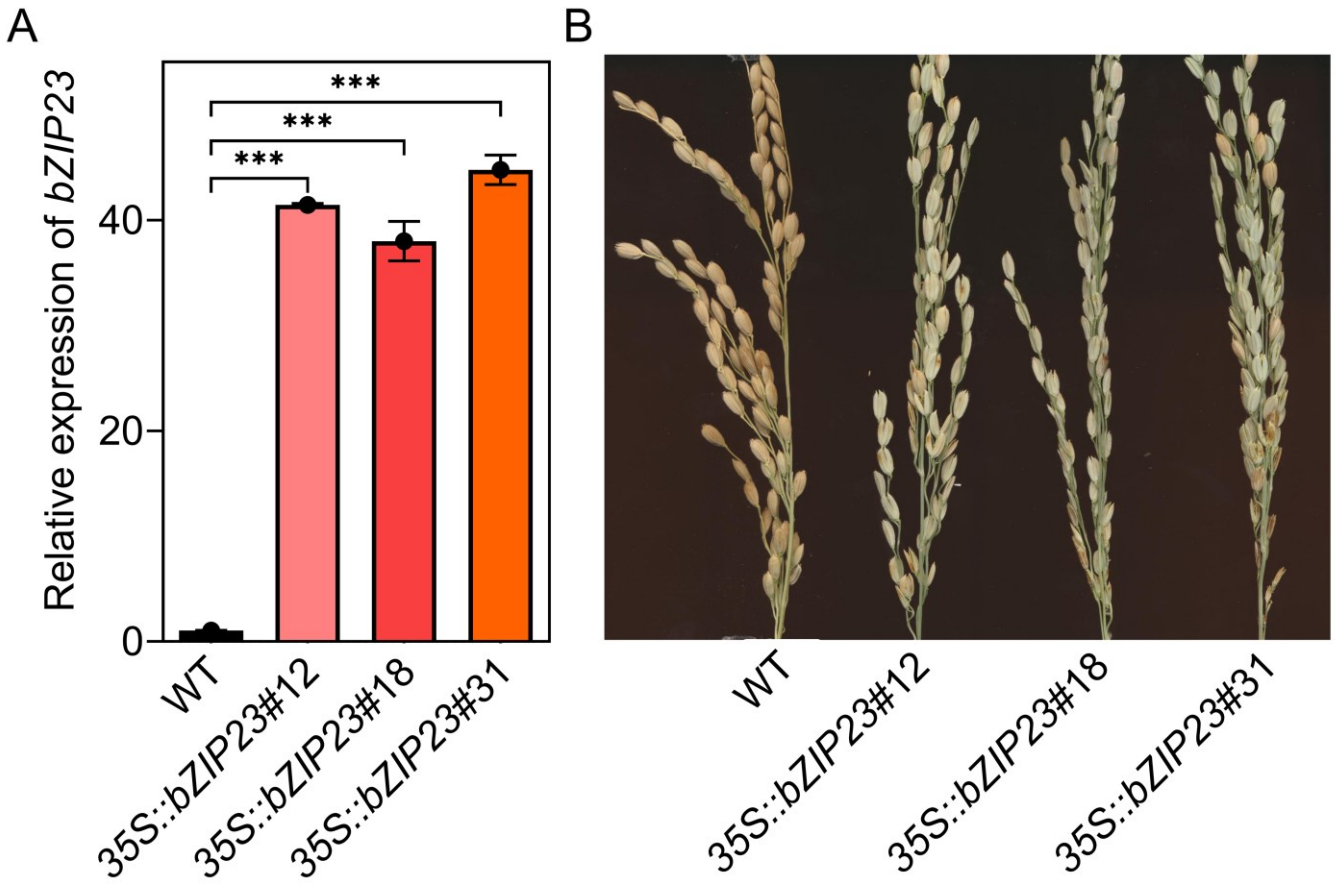

Fig. S9. The *bZIP23* over-expression in Jigeng88. (*A*) Relative expression of *bZIP23* in leaves of WT and *35S::bZIP23* plants. (*B*) Panicles at mature stage of WT and *35S::bZIP23* plants.

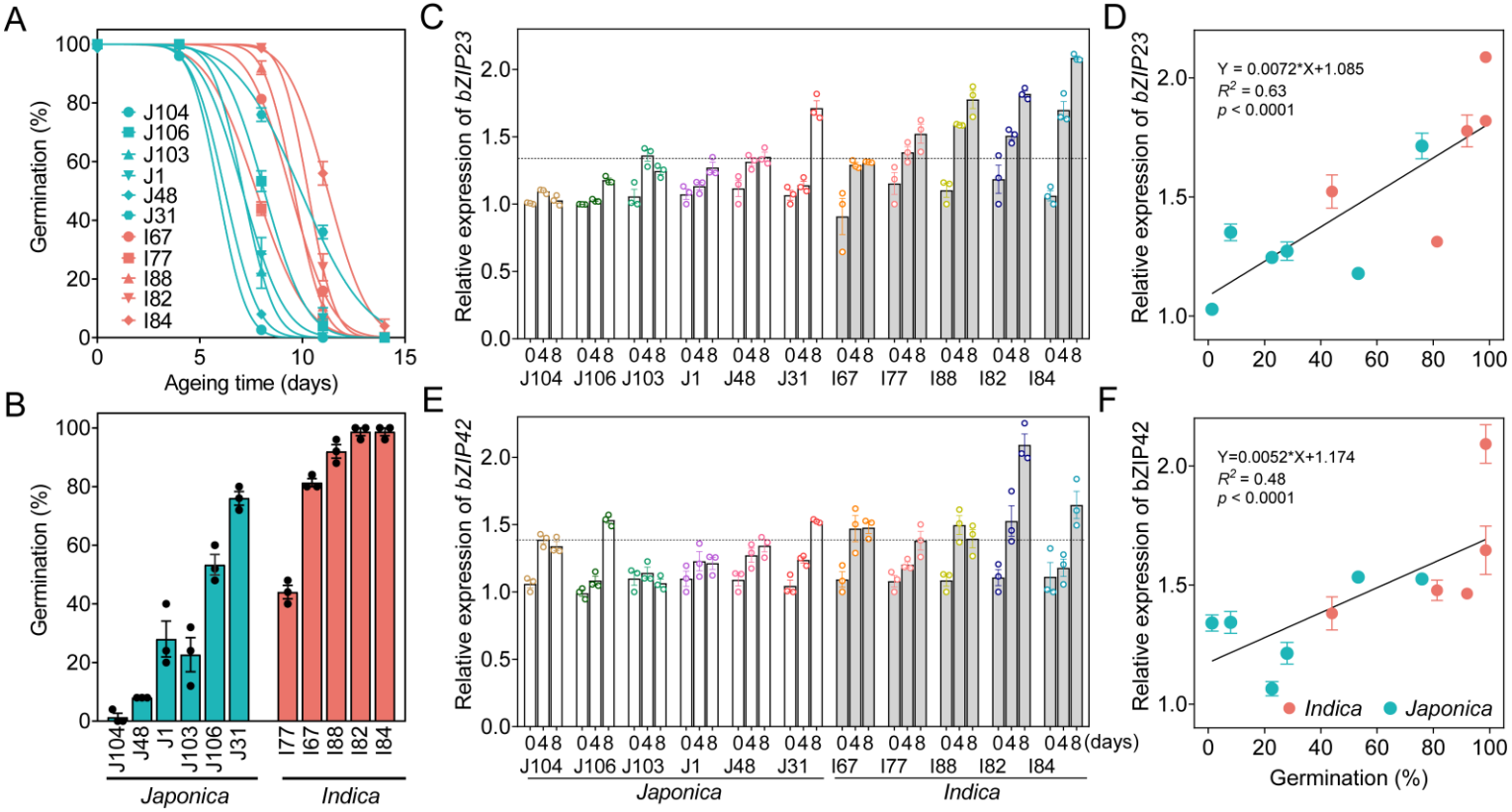

Fig. S10. Correlation of seed vigor with *bZIP23* and *bZIP42* expression. (*A*) Change of seed germination of different rice cultivars during accelerated ageing. Seeds were aged under 45°C and 80% RH for 0, 4, 8, 11 and 14 days. (*B*) Germination of seeds of different rice cultivars after aged for 8 days. Error bars indicate ±se (n = 3). (*C*) and (*E*) Expression of *bZIP23* and *bZIP42* in seeds of different rice cultivars during seed ageing, respectively. Seeds were aged under 45°C and 80% RH for 0, 4 and 8 days and the embryos were then excised for qRT-PCR. (*D*) and (*F*) Linear regressions of seed vigor and relative expression of *bZIP23* and *bZIP42*, respectively. The relative expression of *bZIP23* or *bZIP42* was plotted against seed germination at 8 days of ageing. Error bars indicate ±se (n = 3).

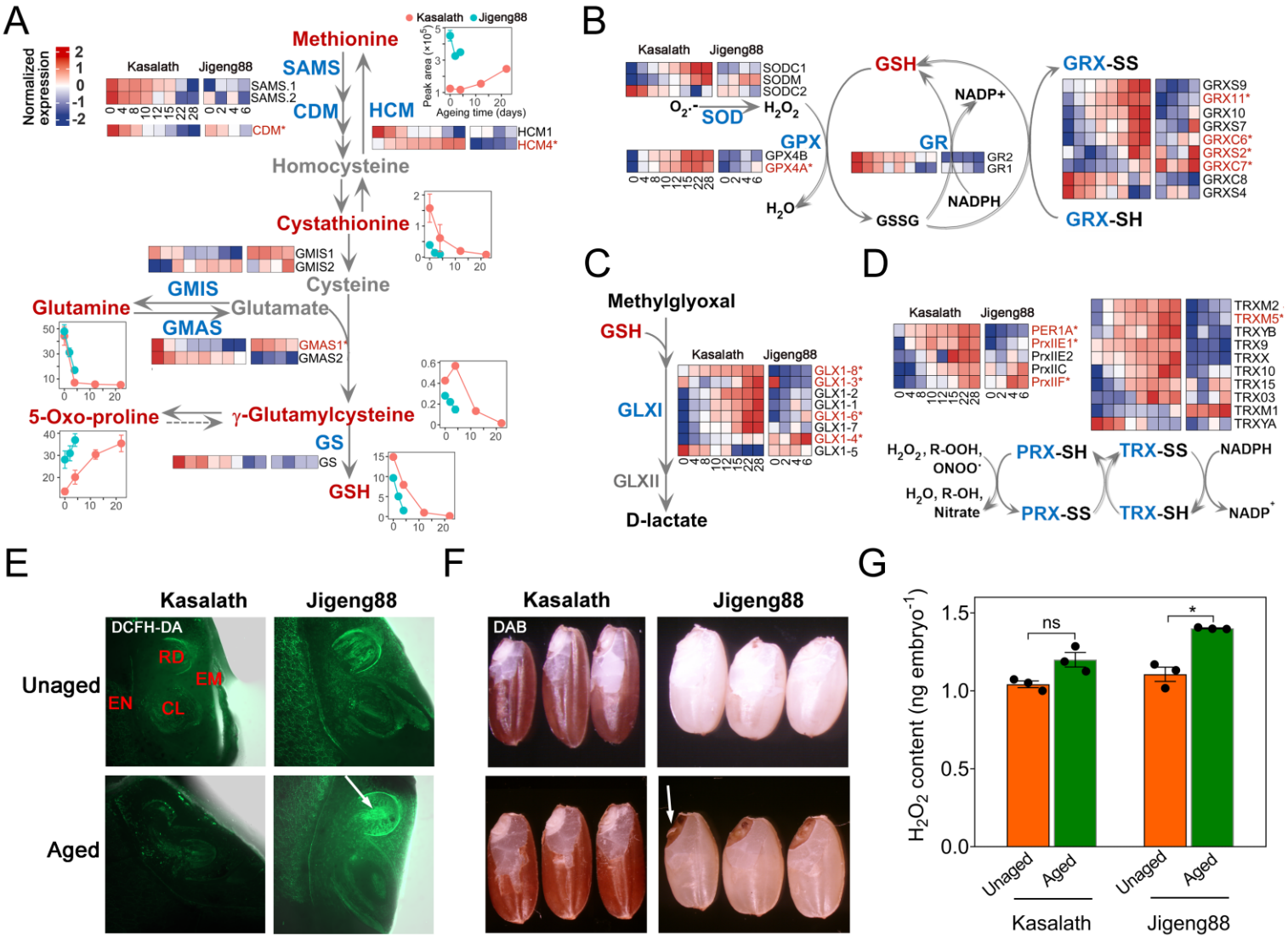

Fig. S11. Varied detoxification ability between Kasalath and Jigeng88 seeds. (*A*) Schematic overview of the glutathione (GSH) biosynthesis pathway alongside gene expression and metabolite accumulation in response to seed ageing. Heat maps show transcripts DE and line plots show metabolites differentially accumulated (DA) during seed ageing. Data in heatmaps are mean values of three biological replicates; in the line plots, data are means±se (n=3). Names of genes DE specifically during Kasalath accelerated ageing and those in common between both two varieties are colored in black and red with asterisk, respectively. No specific DE transcripts were identified during Jigeng88 seed ageing. X-axes of the line plot and heatmap represent days of ageing; y-axis of the line plot represents the metabolite abundance expressed as $\times 10^5$ peak area. SAMS, S-ADENOSYLMETHIONINE SYNTHETASE; CDM, C-5 CYTOSINE-SPECIFIC DNA METHYLASE; HCM, HOMOCYSTEINE S-METHYLTRANSFERASE; GMIS, GLUTAMINE SYNTHETASE; GMAS, GLUTAMATE SYNTHASE; GS, GLUTATHIONE SYNTHETASE. (*B*), (*C*) and (*D*) Schematic overview of detoxification pathways alongside heat maps showing genes DE during seed ageing. Data in heatmaps are mean values of three biological replicates. Gene expression and metabolite accumulation are scaled across all the ageing samples of both Kasalath and Jigeng88 (z score). Gene names are colored as in a. SOD, SUPEROXIDE DISMUTASE; GPX, GLUTATHIONE PEROXIDASE, GR, GLUTATHIONE REDUCTASE; GRX, GLUTAREDOXIN; GLX, GLYOXALASE; PRX, PEROXIREDOXIN; TRX, THIOREDOXIN. (*E*) and (*F*) In situ detection of H_2O_2 during seed ageing using 2',7'-Dichlorodihydrofluorescein diacetate (DCFH-DA) and 3,3'-Diaminobenzidine (DAB) staining agents, respectively. Arrow indicates the production site of H_2O_2. RD, radicle; CL, coleoptile; EM, embryo; EN, endosperm. (*G*) Determination of H_2O_2 content during seed ageing. Kasalath and Jigeng88 seeds were aged, respectively, for four and two days under 45°C and 80% RH at which time cumulative percentage germination was not affected by ageing (Fig. 1b). ns, no significant difference, *, p<0.05. Error bars indicate ±se (n = 3).

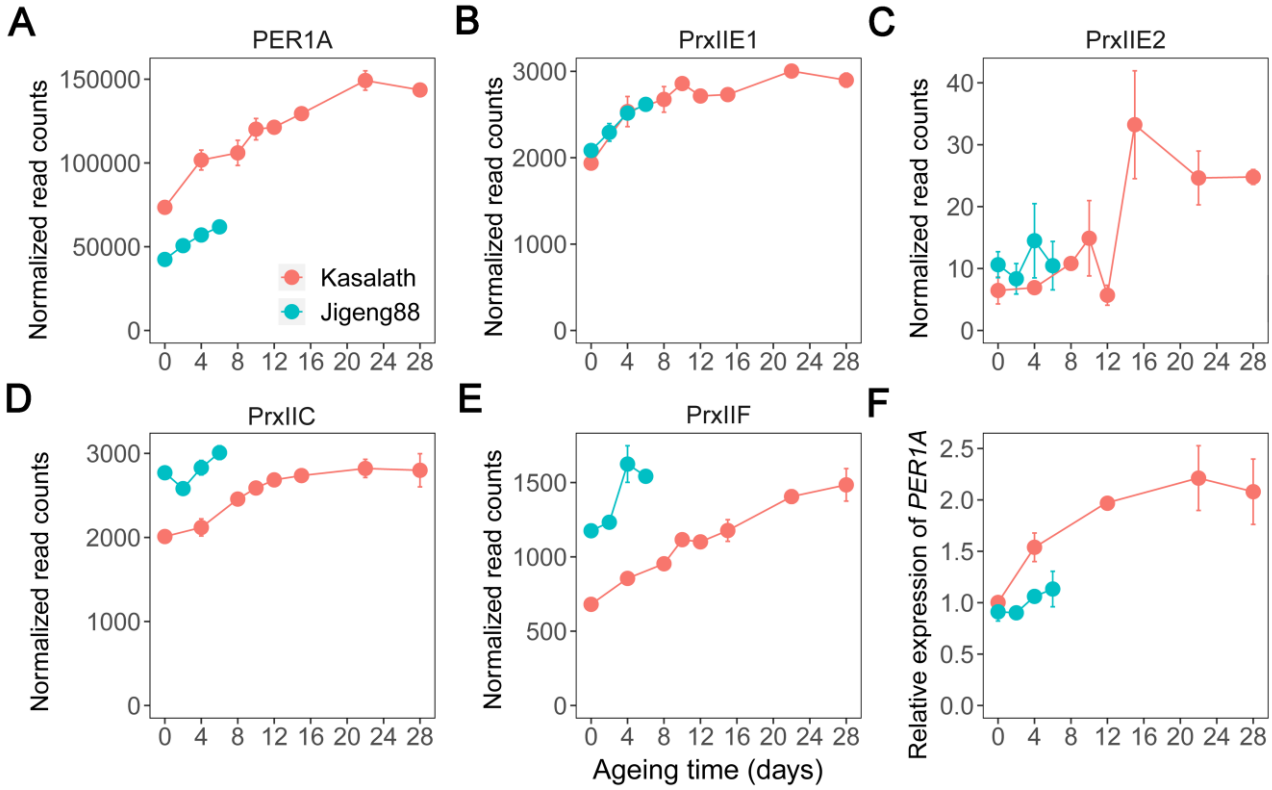

Fig. S12. Peroxiredoxin (PRX) family genes DE during seed ageing. (*A*)-(*E*) Expression profiles of *PRX* family genes during Kasalath and Jigeng 88 seed ageing. Gene expression were quantified by RNA-seq. Read counts are normalized across all the samples from Kasalath and Jigeng88 seeds using DESeq2 program. (*F*) qPCR evaluation of *PER1A* genes expression. Error bars indicate ±se (n = 3).

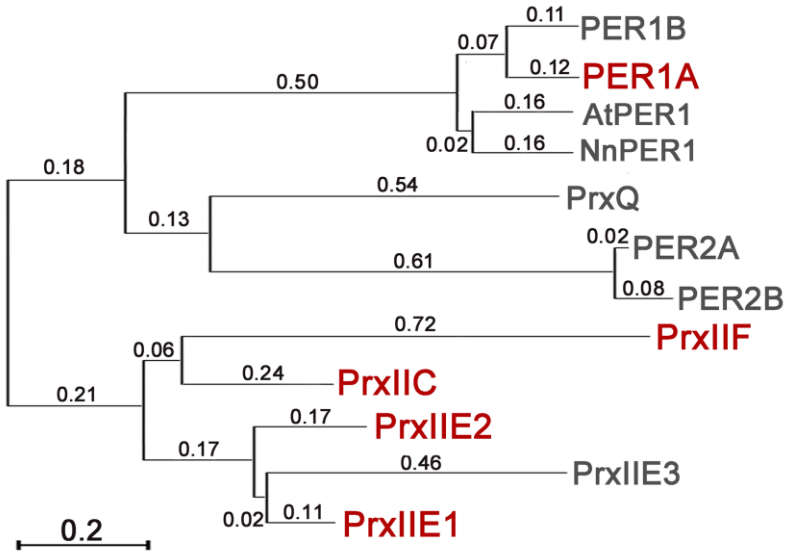

Fig. S13. Phylogenetic tree of rice peroxiredoxin (PRX) family genes. Names colored in red represent genes DE during Kasalath seed ageing.

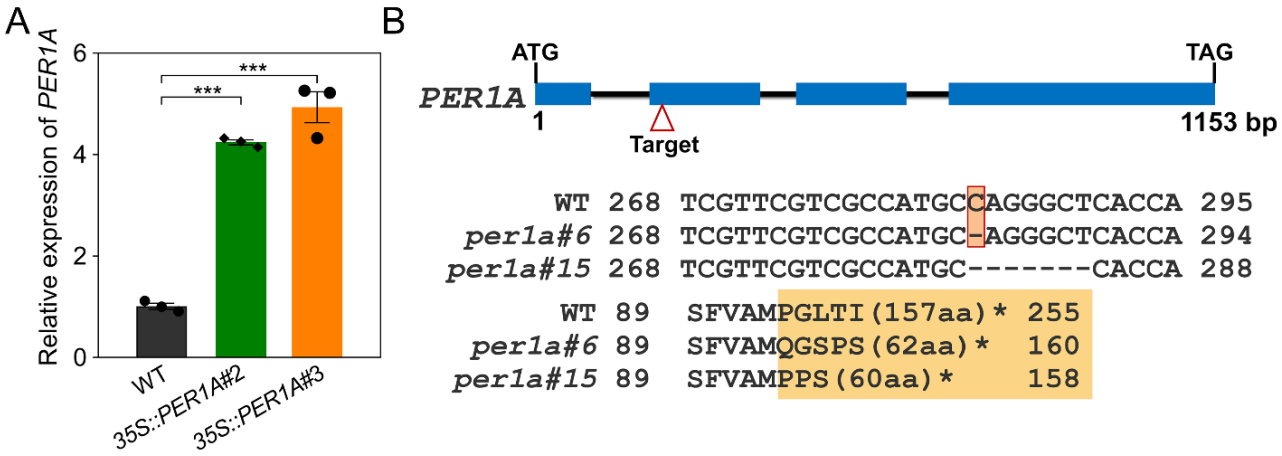

Fig. S14. Genetic modification of *PER1A* in rice. (*A*) Expression of *PER1A* in seeds of wild type (WT) and over-expression transgenic (*35S::PER1A*#2 and *35S:: PER1A*#3) plants. ***, $p < 0.001$ (unpaired t-test). Error bars indicate ±se (n = 3). (*B*) Schematic diagram showing *PER1A* mutation mediated by CRISPR/Cas9. Blue filled box and blank box indicate cDNA and UTR regions, respectively; black line shows intron region. Red triangle shows the target of sgRNA genes. Editing sites on *PER1A* DNA and protein sequence are indicated with orange and yellow boxes, respectively. The omitted amino acids (aa) are indicated in the parenthesis; *, stop codon.

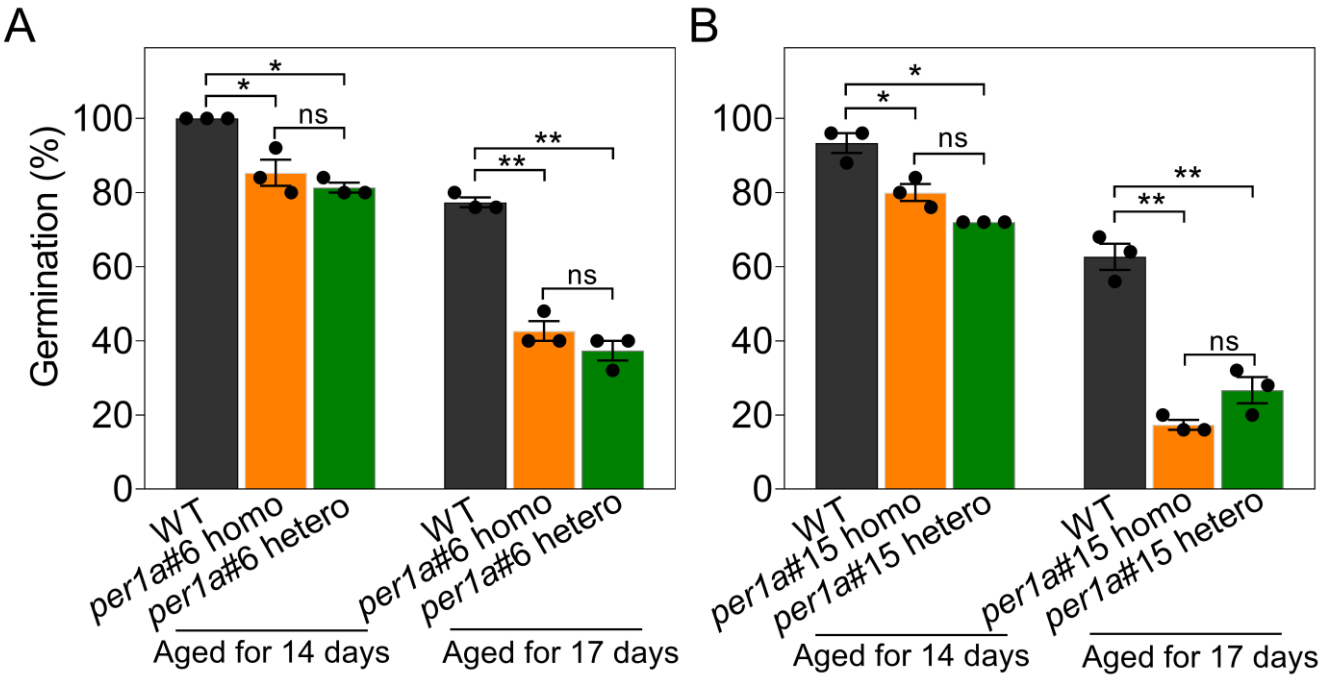

Fig. S15. Germination of WT and *per1a* homozygous (homo) and heterozygous (hetero) seeds after aged for different days. (*A*) and (*B*) show the phenotypes of two different *per1a* lines (*per1a*#6 and #15). Seeds used in (*A*) and (*B*) were harvested from different growing seasons. Seeds were aged under 42°C and 80% RH for 11 and 17 days. ns, no significant difference, *, $p < 0.05$, **, $p < 0.01$ (unpaired t-test). Error bars indicate ±se (n = 3).

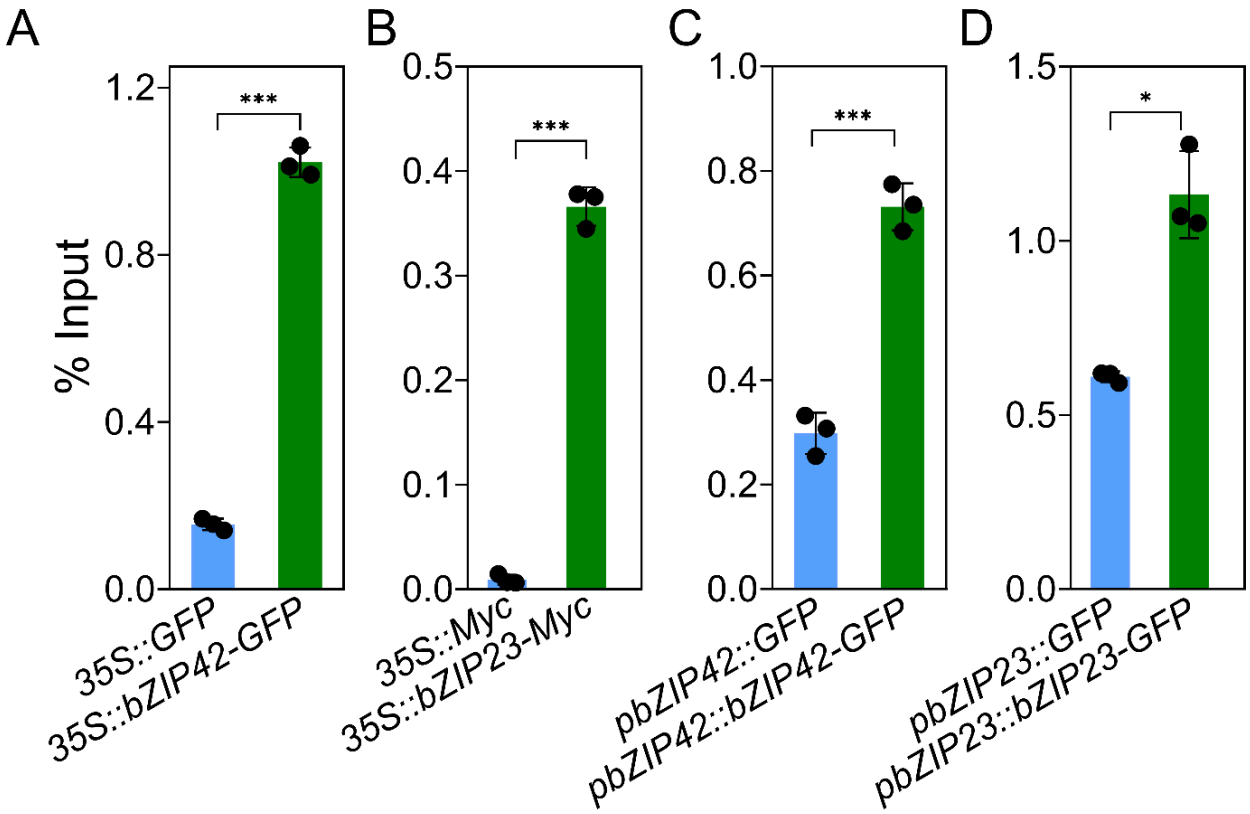

Fig. S16. ChIP-qPCR analysis of relative binding of bZIP23 and bZIP42 to *PER1A* promoter. (*A*) and (*C*) ChIP-qPCR analysis of bZIP42 binding to *PER1A* promoter. (*B*) and (*D*) ChIP-qPCR analysis of bZIP23 binding to *PER1A* promoter. Both 35S and native promoter-driven *bZIP42* or *bZIP23* vectors were constructed and used for the analysis. Anti-GFP affinity bead were used for DNA immune precipitation from *Pro35S:bZIP42-GFP, pbZIP42:bZIP42-GFP* and *pbZIP23:bZIP23-GFP* transgenic rice protoplasts and anti-c-Myc agarose were used for *Pro35S:bZIP23-MYC* transgenic rice protoplasts. *, $p < 0.05$, ***, $p < 0.001$ (unpaired t-test). Error bars indicate ±se (n = 3).

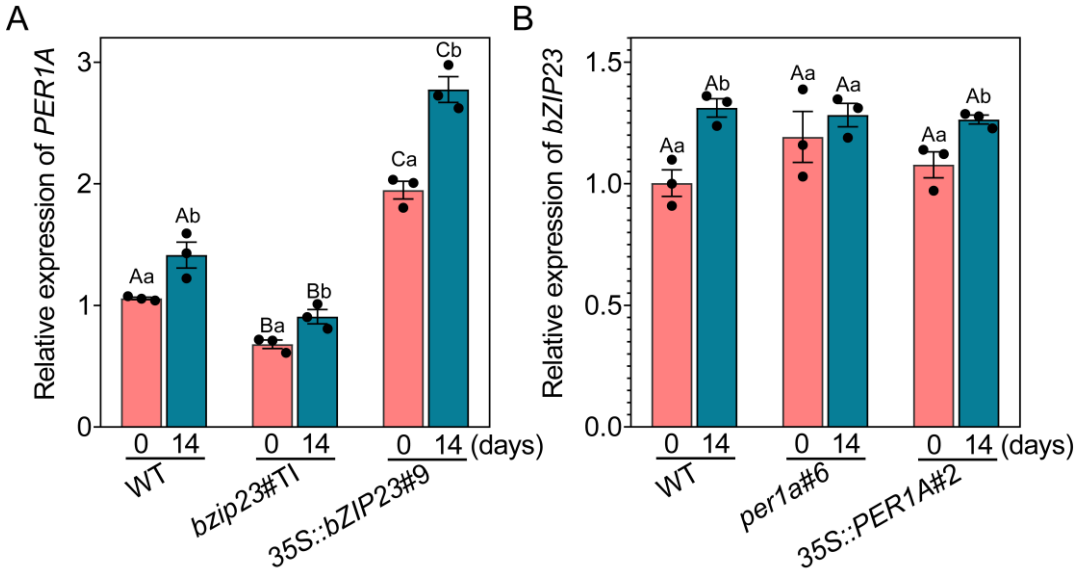

Fig. S17. Determination of genetic relationship between bZIP23 and PER1A. (*A*) Expression of *PER1A* in seeds of wild type (WT) and *bZIP23* T-DNA insertion (*bzip23*#TI) and over-expressed (*35S::bZIP23*#9) plants before and after ageing. (*B*) Expression of *bZIP23* in seeds of wild type (WT) and *PER1A* knockout (*per1a*#6) and over-expressed (*35S::PER1A*#2) plants before and after ageing. Seeds were aged at 42°C and 80% RH for 0 and 14 days and the embryos were excised for RNA extraction and qRT-PCR analysis. Different lowercase letters above the bar indicate significant difference ($p < 0.05$, unpaired t-test) between seeds of different genotypes at a given ageing time; different uppercase letters indicate significant difference ($p < 0.05$, unpaired t-test) between unaged and aged seeds within a given genotype. Error bars indicate ±se (n = 3).

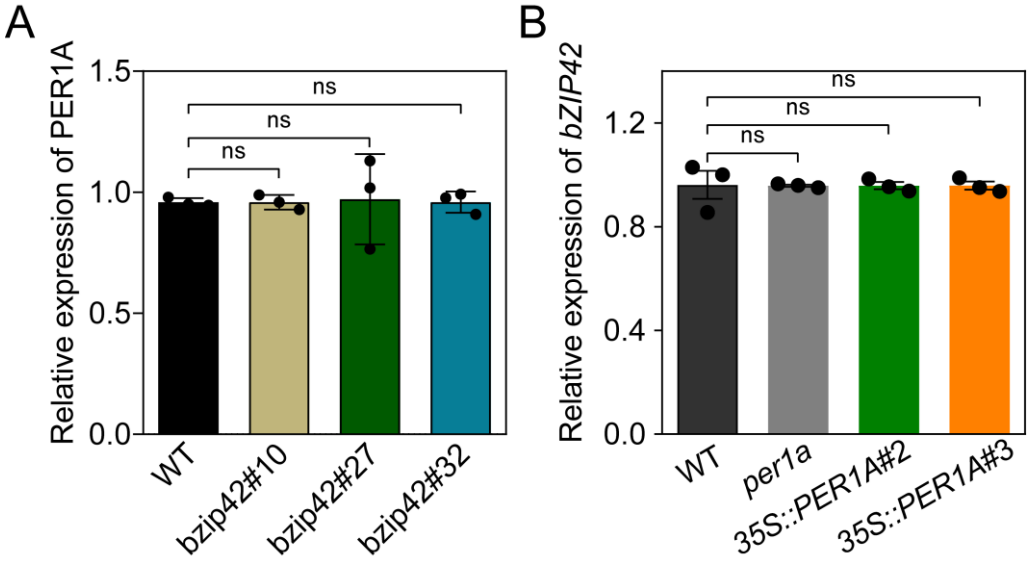

Fig. S18. Determination of genetic relationship between b*ZIP42 and PER1A*. (*A*) Expression of *PER1A* in seeds of wild type (WT) and *bZIP42* CRISPR knockout (*bzip42*#10*, bzip42*#27 and *bzip42*#32) plants. (*B*) Expression of *bZIP42* in seeds of WT, *PER1A* CRISPR knockout (*per1a*) and over-expressed (*35S::PER1A*#2 and *35S::PER1A*#3) plants. Error bars are ±se (n = 3). ns, no significant difference.

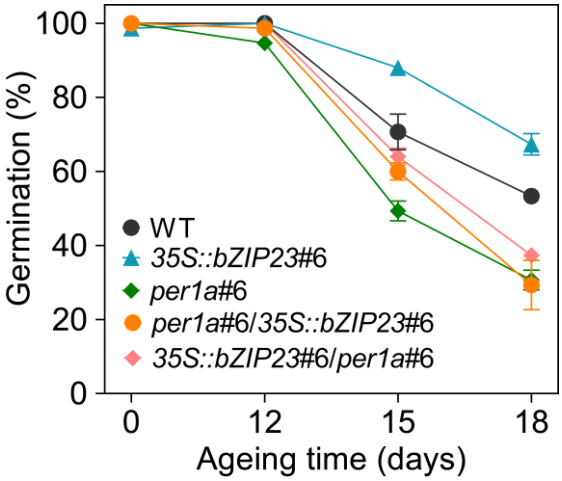

Fig. S19. Change in germination of WT, *35S::bZIP23*#6, *per1a*#6, *35S::bZIP23*#6/*per1a*#6 and *per1a*#6 /*35S::bZIP23*#6 seeds during accelerated ageing. Seeds were aged under 42°C and 80% for 0, 12, 15 and 18 days. Error bars indicate ±se (n = 3).

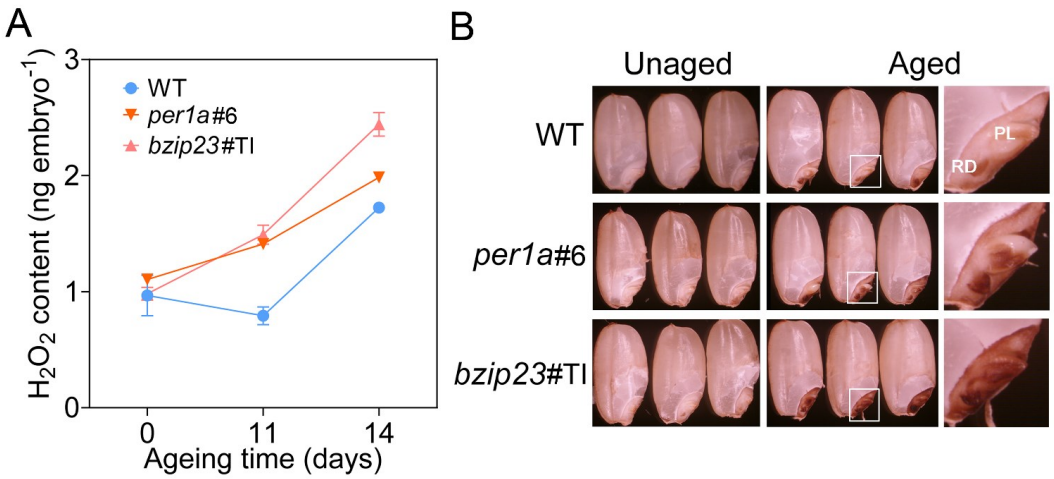

Fig. S20. Accumulation of H_2O_2 during ageing of WT, *bzip23* and *per1a* seeds. (*A*) Change of H_2O_2 content during ageing of WT, *bzip23* and *per1a* seeds. Error bars indicate ±se (n = 3). (*B*) In situ detection of H_2O_2 during ageing of WT, *bzip23* and *per1a* seeds using 3,3‘-Diaminobenzidine (DAB) staining agents. The rightmost panel showed a representative embryo enlarged from the seeds indicated with the white frame. RD, radicle, PL, plumule.

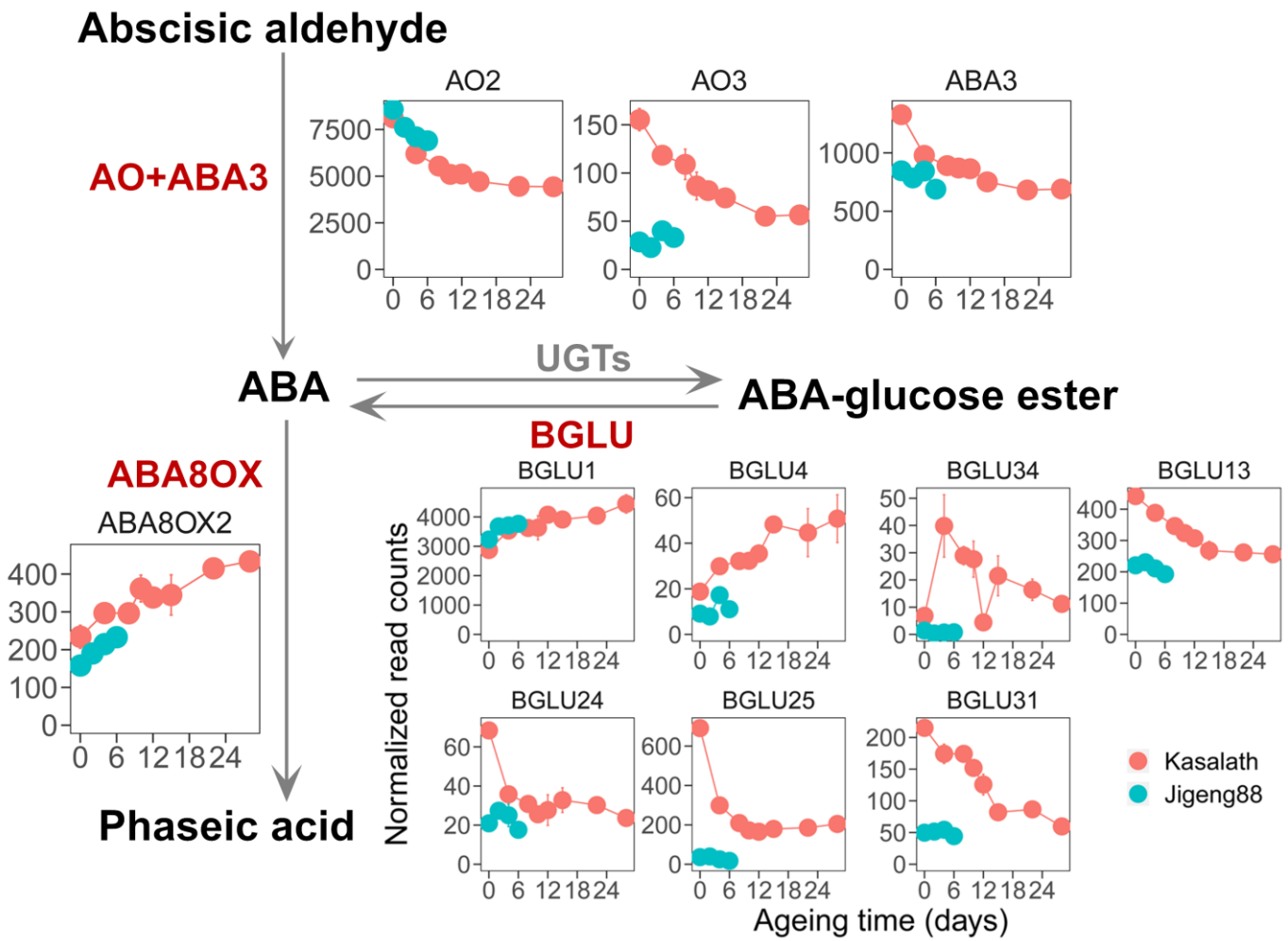

Fig. S21. Schematic overview of ABA metabolism alongside differentially expressed (DE) gene expression during seed ageing. AO, aldehyde oxidase; ABA3, molybdenum cofactor sulfurase; ABA8OX, abscisic acid 8'-hydroxylase; BGLU, beta-glucosidase. No UDP-glucosyltransferases (UGTs) were detected to be differentiated expressed during seed ageing. x-axis of line plot is the ageing time; y-axis is the normalized read counts.

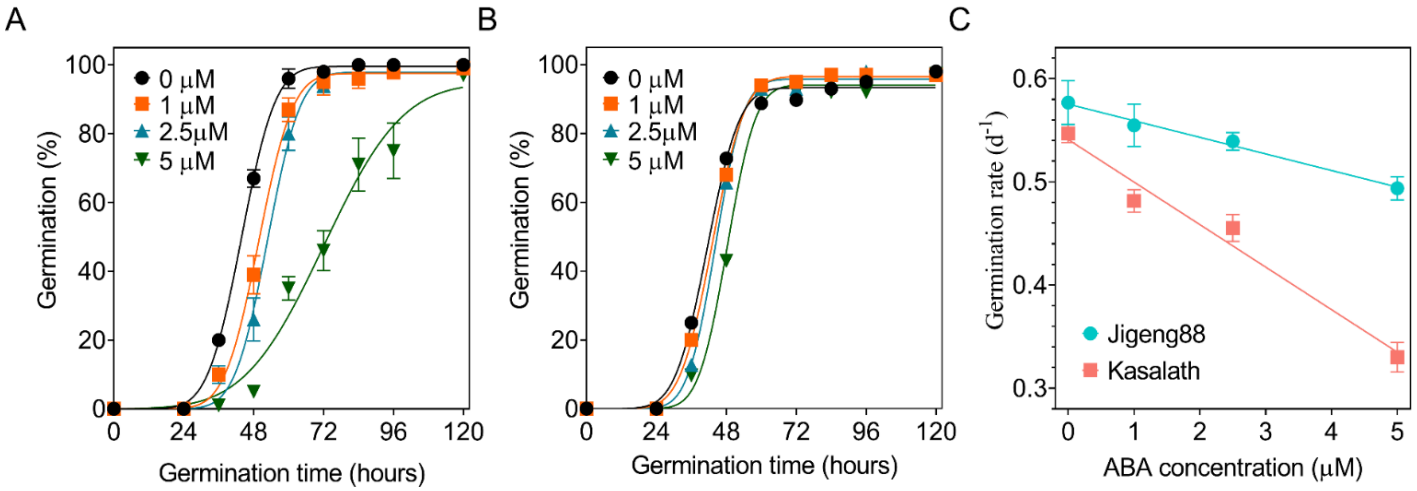

Fig. S22. Variation of sensitivity of Kasalath and Jigeng88 seeds to ABA treatment. (*A*) Time courses of germination of Kasalath seeds treated with different concentration of ABA. (*B*) Time courses of germination of Jigeng88 seeds treated with different concentration of ABA. (*C*) Change of germination rates of Kasalath and Jigeng88 seeds with ABA concentration increased. Germination rate was defined as reverse time to germinate to 50%.

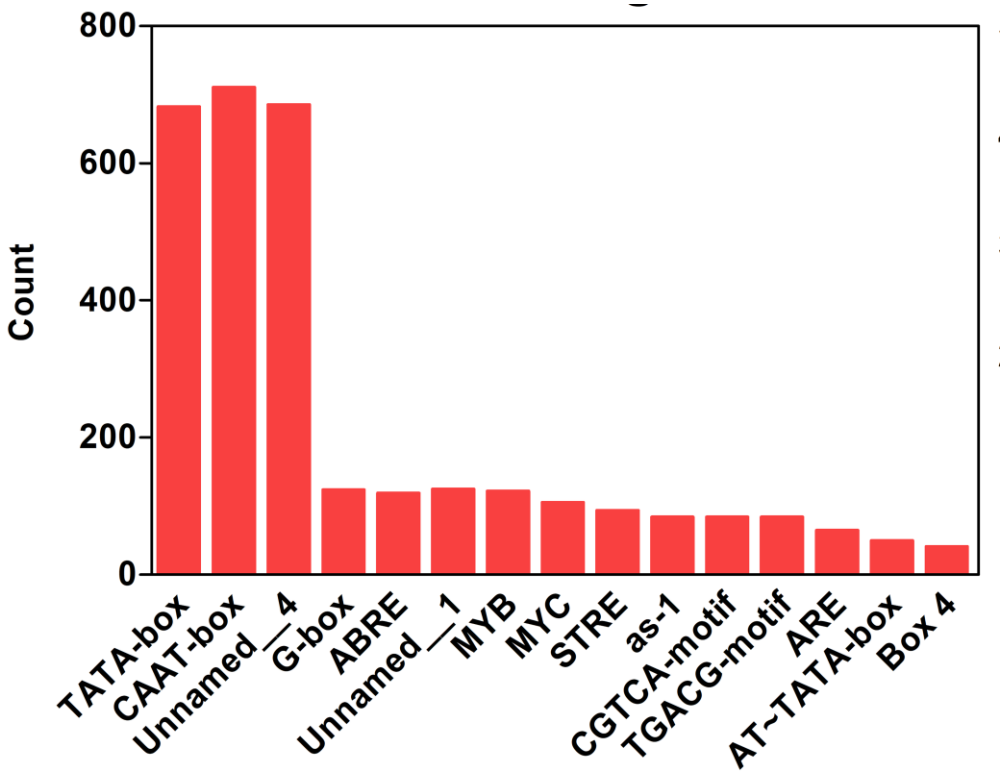

Fig. S23. Top 15 abundant cis-elements predicted to be located in the promoters of detoxification-related genes. The prediction was performed on 1500 bp promoter upstream of ATG of genes using PlantCARE web service (http://bioinformatics.psb.ugent. be/webtools/plantcare/html/).

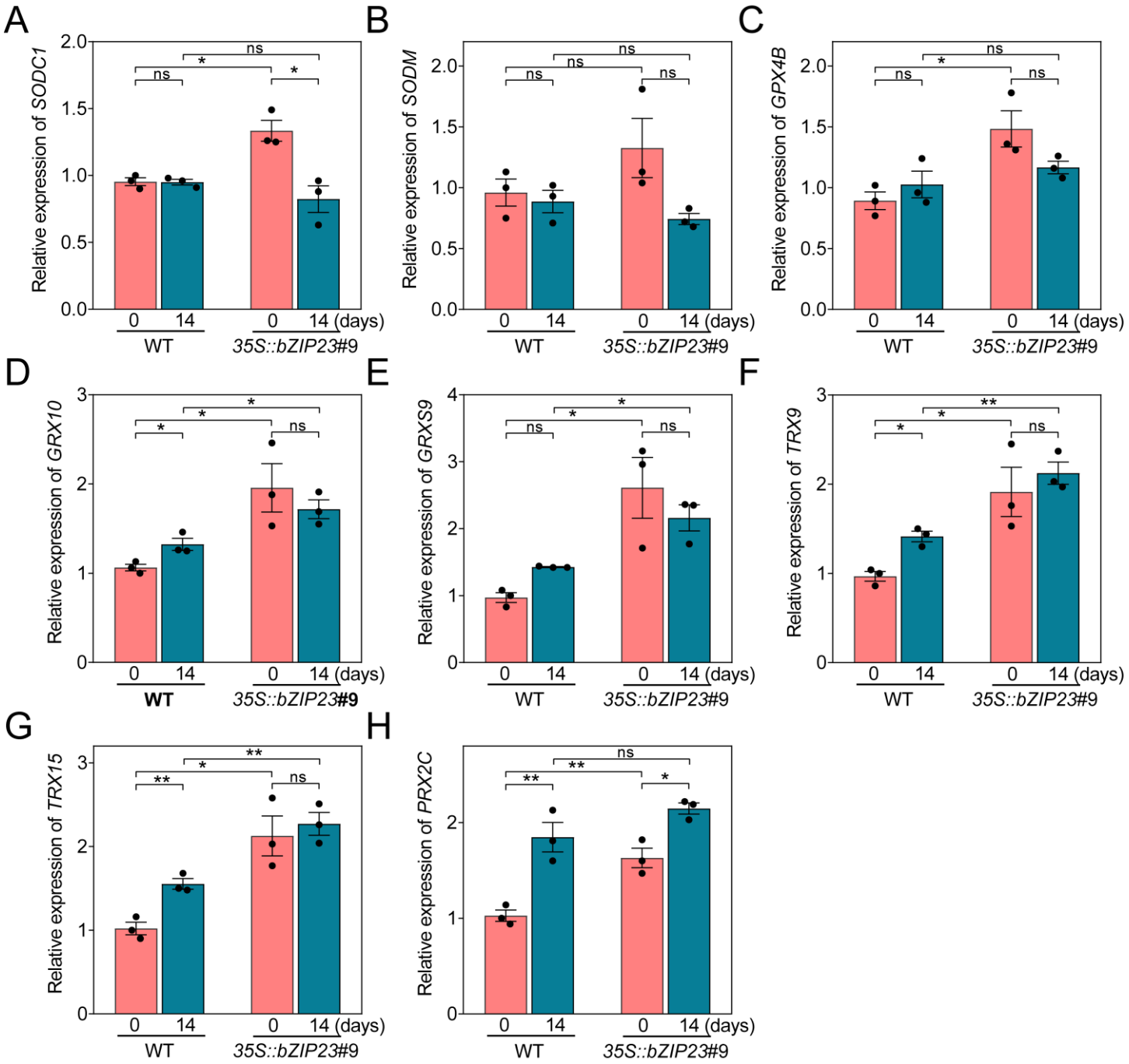

Fig. S24. Expression of genes related to ROS detoxification in seeds of wild type (WT) and *bZIP23* over-expressed (*35S::bZIP23*#6) plants before and after ageing. WT and *35S::bZIP23*#9 seeds were aged at 42°C and 80% RH for 0 and 14 days and then the embryo were excised for RNA extraction and gene expression analysis. Eight genes of *SODC1* (*A*), *SODM* (*B*), *GPX4B* (*C*), *GRX10* (*D*), *GRXS9* (*E*), *TRX9* (*F*), *TRX15* (*G*) and *PRX2C* (*H*) involved in different pathways of ROS detoxification (see Fig. S11) were chose for the analysis. ns, no significant difference, *, $p < 0.05$, **, $p < 0.01$ (unpaired t-test). Error bars indicate ±se (n = 3).

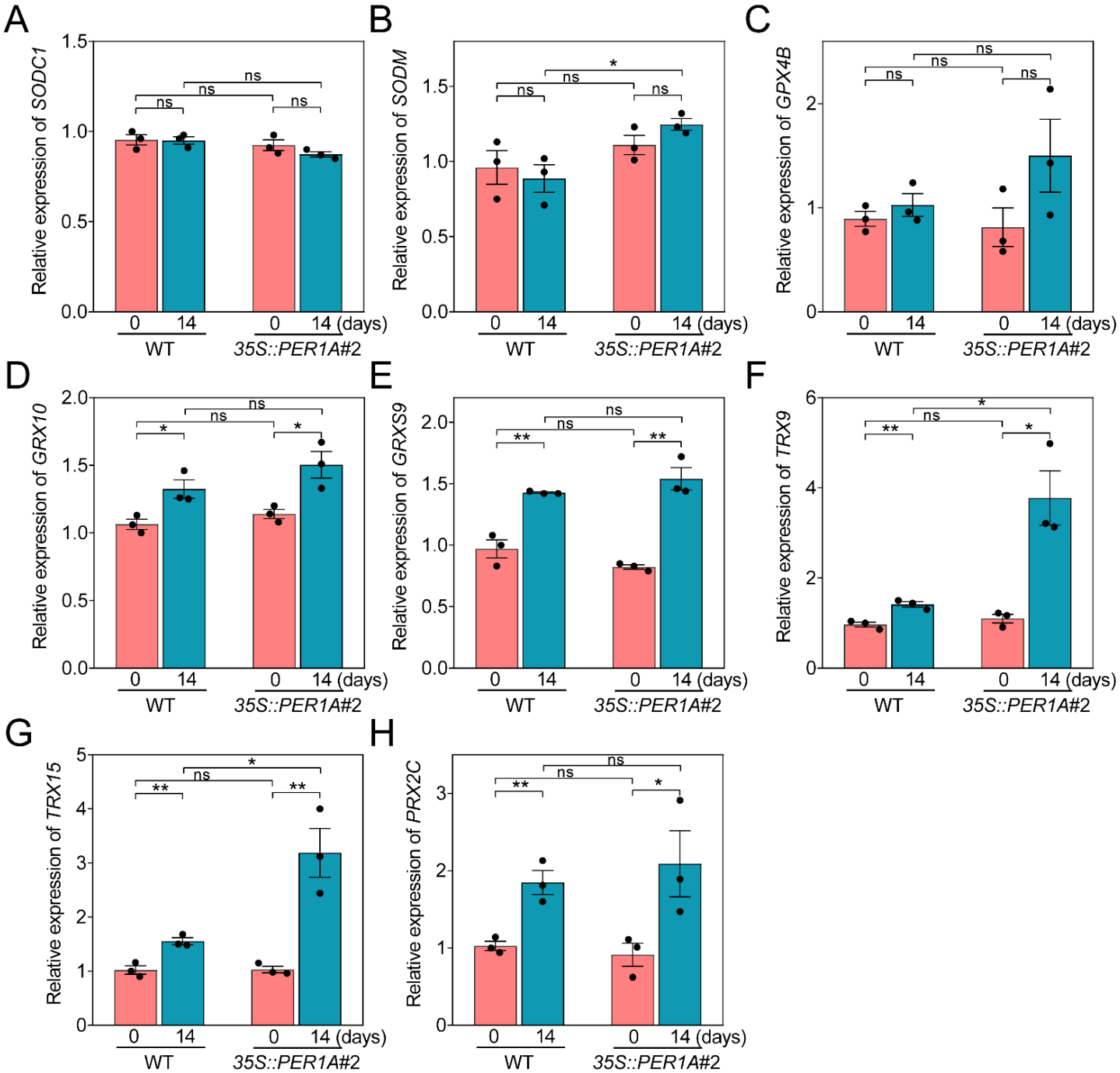

Fig. S25. Expression of genes relatedto ROS detoxification in seeds of wild type (WT) and *PER1A* over-expressed (*35S::PER1A*#2) plants before and after ageing. WT and *35S::PER1A*#2 seeds were aged at 42°C and 80% RH for 0 and 14 days and then the embryo were excised for RNA extraction and gene expression analysis. Eight genes of *SODC1* (*A*), *SODM* (*B*), *GPX4B* (*C*), *GRX10* (*D*), *GRXS9* (*E*), *TRX9* (*F*), *TRX15* (*G*) and *PRX2C* (*H*) involved in different pathways of ROS detoxification (see Fig. S11) were chose for the analysis. ns, no significant difference, *, $p < 0.05$, **, $p < 0.01$ (unpaired t-test). Error bars indicate ±se (n = 3).

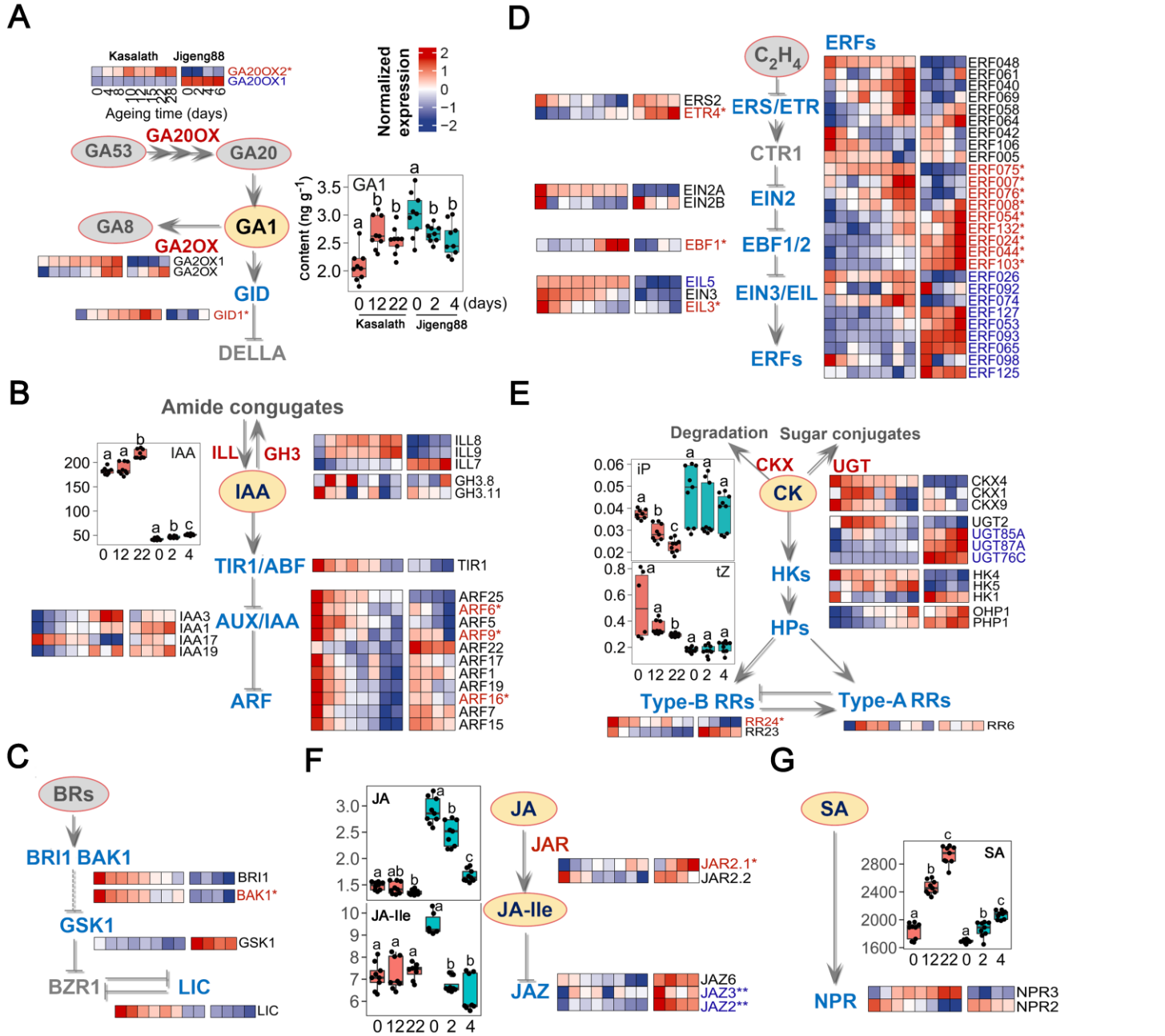

Fig. S26. Involvement of multiple hormone pathways in response to seed ageing. (*A*), (*B*), (*C*), (*D*), (*E*), (*F*) and (*G*) Schematic overviews of gibberelin (GA), auxin, brassinosteroid (BR), ethylene (C_2H_4), cytokinin (CK), Jasmonate acid (JA) and salicylic acid (SA) metabolism and/or signaling pathway alongside gene expression or hormone level change. Arrows shows the downstream reaction of the metabolism or the promotion actions of the signaling pathway; bar ends show the inhibitory actions of the pathway. In panel c, the dashed line indicates multiple processes involved in the pathway. Heat maps show the expression of transcripts DE during seed ageing; box plots show the change of hormone level during seed ageing. Columns of heat maps represent time points of seed ageing. x-axis of boxplots is the ageing time and y-xis is the hormone content (ng per g seeds), which are indicated as an example in panel a. Genes identified to be DE (FDR < 0.01) during Kasalath, both two varieties or Jigeng88 are colored in black, red with asterisk and blue, respectively. In the boxplots, letters above the boxes indicate significant difference ($p < 0.05$) of hormone level among different ageing time points of each variety. Gene expression are scaled across all the samples from Kasalath and Jigeng88 seeds (z score). Data at each ageing time points are the means of three replicates. GA20OX, gibberellin 20 oxidase; GA2OX, gibberellin 2-beta-dioxygenase; GID, gibberellin receptor; ILL, IAA-amino acid hydrolase ILR1-like; GH3, indole-3-acetic acid-amido synthetase; TIR1/ABF, transport inhibitor response1/auxin signaling f-box; AUX/IAA, auxin/indole-3-acetic acid transcriptional repressors; ARF, auxin response factor; BRI1, brassinosteroid insensitive 1 ; BAK1, BRI1 Associated receptor Kinase 1; GSK1, Glycogen Synthase Kinase 1; BZR1, BZR1/BES1 family transcription factor; LIC, tiller angle increased controller; ERS/ETR, Ethylene response sensor /ETHYLENE RESPONSE; EIN2, Ethylene-insensitive protein 2; EBF, EIN3 Binding F-box protein; EIN3/EIL, ethylene-insensitive protein/ ethylene-insensitive lke protein; ERF, ethylene response factor; CKX, ck oxidase/dehydrogenase; UGT, udp glucosyltransferase; HK, histidine kinase; HP, histidine phosphotransfer; Type- A/B RRs, Type-A/B response regulators; JAR, Jasmonic acid-amido synthetase; JA-Ile, jasmonoyl-isoleucine; JAZ, jasmonate-zim domain protein; NPR, nonexpresser of pathogenesis-related protein.

Table S1. List of rice cultivars for assessment of seed vigor and bZIP23 and bZIP42 expression.

ID	Cultivars	Subspecies
J1	Zhonghua11	Japonica
J31	Koshihikari	Japonica
J48	Carolina gold sel	Japonica
J103	Belle patna	Japonica
J104	Botpa bara	Japonica
J106	Chigyungdo	Japonica
I67	Dheki shaita	Indica
I77	Hegra	Indica
I82	Kalia	Indica
I84	Kele bardhan	Indica
I88	Lakhi puri	Indica

Table S2. Primers used for cloning full-length of *PER1A*, *bZIP23* and *bZIP42* cDNA sequence

Genes	Forward primer (5'-3')	Reverse primer (5'-3')
PER1A	AAGCTTATGGACGGTCATGGGGATG	TCTAGACTAGCCGACCTTGGTGAAG
bZIP23	TCGACTCTAGAAAGCTTATGGATTTTCCGGGAG	GTACCGGATCCACTAGTCCATGGACCCGTCAGA
bZIP42	CAGGGTACCCGGGGATCCATGATTCAGGCAATGGCTTC	CATGGTACTAGTGTCGACGAAGGCGGCCGAGCTTGTT

Table S3. Primers used for qPCR evaluation of gene expression quantified by RNA-seq.

Genes	Forward primer (5'-3')	Reverse primer (5'-3')
PER1A	TAAGGCAGCACAGTCGTTCGT	GAAGTCGTGGATGCGGATCTTG
bZIP23	GCTGAACGATGAACTCCAGAA	CTTTGCTGTCGGTCCAACTT
bZIP42	GCAACTCACCTGGCACCTCA	CTGCTTCCTCGCTCTTGACCT
GAPDH	CTCCTCTCGCCAAGGTCATCAATG	TTCCACCTCTCCAGTCCTTCATCG
GPX4B	CTCAAGGTTACTGTTGCAAACA	GGCAGCTCATCGACAATTTTAT
GRXS9	GCTCGAGGATTAGATCTCGTAC	CACTATTGAGCATCCCATAGGT
GRX10	CGTATGAAGAGGCTCTCTCAAA	TTAGCATGACAAAGTTGACACG
PRX2C	CCTTTGAACTGATAGGCTTGTG	AACTCTGAAGTCTGAACCACAT
TRX9	CTCTGAATCAACAACGCAGTAG	GGACACACACTTCTCCTAATCA
TRX15	CATCTACTCCAAGTCCTGGTG	CTAACACCTTTTGCAACTGAGG
SODC1	TCGCCTCCTCCTTCATCCTCCT	GCCCTTAACAATCTCACTGCTACCAA
SODM	CTCGCTGATAGGCTTGAGGTTATTCC	CCACCTACGTCGCCAACTACAAC

Table S4. Primers used for amplification of PER1A promoter and its putative binding transcriptional factors in Y1H experiments.

Genes	Forward primer (5'-3')	Reverse primer (5'-3')
PER1A promoter	GAATTCGAGCTCGGTACCTGGTGAA CTTAGGGCCTG	TGCCTCGAGGTCGACCGACGAACG ACTGTGCTG
bZIP23	GATTATGCCTCTCCCGAATTCATGG ATTTTCCGGGAGGGAGCG	AGAAGTCCAAAGCTTCTCGAGTCAC CATGGACCCGTCAGAGTC
bZIP42	GATTATGCCTCTCCCGAATTCATGAT TCAGGCAATGGCTTCGC	AGAAGTCCAAAGCTTCTCGAGTCAG AAGGCGGCCGAGCTTG

Table S5. Primers used for qPCR analysis of enrichment of bZIP23 and bZIP42 binding to PER1A promoter

Genes	Forward primer (5'-3')	Reverse primer (5'-3')
bZIP23	TCGACTCTAGAAAGCTTATGGATTTTCCGGGAG	GTACCGGATCCACTAGTCCATGGACCCGTCAGA
bZIP42	CAGGGTACCCGGGGATCCATGATTCAGGCAATGGCTTC	CATGGTACTAGTGTCGACGAAGGCGGCCGAGCTTGTT
PER1A fragment	AATGGACGGTCATGGGGAT	TGGAGACTGGAGTGAGATC
Actin1 fragment	TGTTGGCATGGAGTGCTTTGAC	GGCTGACACCATCACCAGAGT
bZIP23 promoter	AGCTATGACCATGATTACGAATTCCCGCGCGCAGGCCGCTGTCAGGCG	GACTCTAGAGGATCCCCGGGTACCCTCCAAACTCCAACCAACCAATCC
bZIP42 promoter	AGCTATGACCATGATTACGAATTCAGCTCCACCTCTTCTCTTGTTC	GACTCTAGAGGATCCCCGGGTACCGAATCGGCGCTCTCAATTACAC

Table S6. Primers used for construction of protein expression vectors for EMSA.

Genes	Forward primer (5'-3')	Reverse primer (5'-3')
bZIP23	GCCATGGCTGATATCGGATCCATGG ATTTTCCGGGAGGGAGCG	CTCGAGTGCGGCCGCAAGCTTTCAC CATGGACCCGTCAGAGTC
bZIP42	GCCATGGCTGATATCGGATCCATGAT TCAGGCAATGGCTTCGC	CTCGAGTGCGGCCGCAAGCTTTCAG AAGGCGGCCGAGCTTG

Table S7. Primers used for amplification of PER1A promoter and its putative binding transcriptional factors in DLR experiments.

Genes	Forward primer (5'-3')	Reverse primer (5'-3')
PER1 promoter	GACGGTATCGATAAGCTTCGATATGG CGGTGTGAAGGTCTG	TCTAGAACTAGTGGATCCCGACGAA CGACTGTGCTG
bZIP23	GTGGATCCCCCGGGCTGCAGATGGA TTTTCCGGGAGGGAGCG	GATTTCAGCGAATTGGTACCTCACC ATGGACCCGTCAGAGTC
bZIP42	GTGGATCCCCCGGGCTGCAGATGAT TCAGGCAATGGCTTCGC	GATTTCAGCGAATTGGTACCTCAGA AGGCGGCCGAGCTTG

Dataset S1. Summary of read counts, quility control and read alignment of RNA-seq. Alignment of reads were performed using the Hisat program

Dataset S2. List of transcripts differentially expressed between Kasalath and Jigeng88 unaged seeds

Dataset S3. List of transcripts differentially expressed during Kasalath and Jigeng88 seed ageing. Functiona category and sub category were manually annotated according to Bevan et al. (2).

Dataset S4. List of metabolites quantified in Kasalath and Jigeng88 seeds.

Dataset S5. List of metabolites differentially accumulated during Kasalath and Jigeng88 seed ageing.

Dataset S6. List of transcriptional factors possess over-representative targets among the genes differentially expressed during Kasalath and Jigeng88 seed ageing.

Dataset S7. Prediction of cis-element in promoter of DE genes involved in detoxification using PlantCARE. Promoter sequence was -1500 bp from ATG. ABRE element related to ABA signal was predicted to be exist in almost all the genes.

SI References

1. Y. Xiang, N. Tang, H. Du, H. Y. Ye, L. Z. Xiong, Characterization of OsbZIP23 as a key player of the basic leucine zipper transcription factor family for conferring abscisic acid sensitivity and salinity and drought tolerance in rice. *Plant Physiol.* **148**, 1938-1952 (2008).
2 M. Bevan *et al.*, Analysis of 1.9 Mb of contiguous sequence from chromosome 4 of *Arabidopsis thaliana*. *Nature* **391**, 485-488 (1998).